

Enhancing the discrimination accuracy between metastases, gliomas and meningiomas on brain MRI by volumetric textural features and ensemble pattern recognition methods

Pantelis Georgiadis^{a,*}, Dionisis Cavouras^b, Ioannis Kalatzis^b, Dimitris Glotsos^b,
Emmanouil Athanasiadis^a, Spiros Kostopoulos^a, Koralia Sifaki^c, Menelaos Malamas^c,
George Nikiforidis^a, Ekaterini Solomou^d

^aMedical Image Processing and Analysis (MIPA) Group, Laboratory of Medical Physics, School of Medicine, University of Patras, Rio GR-26503, Greece

^bMedical Image and Signal Processing Laboratory, Department of Medical Instruments Technology, Technological Educational Institute of Athens, Aigaleo, Athens GR-12210, Greece

^c251 General Hellenic Airforce Hospital, MRI Unit, Katerhaki, Athens GR-11525, Greece

^dDepartment of Radiology, School of Medicine, University of Patras, Rio GR-26503, Greece

Received 4 February 2008; revised 20 May 2008; accepted 21 May 2008

Abstract

Three-dimensional (3D) texture analysis of volumetric brain magnetic resonance (MR) images has been identified as an important indicator for discriminating among different brain pathologies. The purpose of this study was to evaluate the efficiency of 3D textural features using a pattern recognition system in the task of discriminating benign, malignant and metastatic brain tissues on T_1 postcontrast MR imaging (MRI) series. The dataset consisted of 67 brain MRI series obtained from patients with verified and untreated intracranial tumors. The pattern recognition system was designed as an ensemble classification scheme employing a support vector machine classifier, specially modified in order to integrate the least squares features transformation logic in its kernel function. The latter, in conjunction with using 3D textural features, enabled boosting up the performance of the system in discriminating metastatic, malignant and benign brain tumors with 77.14%, 89.19% and 93.33% accuracy, respectively. The method was evaluated using an external cross-validation process; thus, results might be considered indicative of the generalization performance of the system to “unseen” cases. The proposed system might be used as an assisting tool for brain tumor characterization on volumetric MRI series.

© 2009 Elsevier Inc. All rights reserved.

Keywords: Brain tumors; MRI; Volumetric textural features; Pattern classification

1. Introduction

The subjective nature of many of the decisions related with the process of brain tumor characterization has led clinicians to continuously seek for greater accuracy in the characterization of brain tumor tissues, mainly from magnetic resonance imaging (MRI) findings [1]. The introduction of pattern recognition techniques has enabled experts to extract diagnostic information from the displayed texture on MR

images. However, most of the proposed pattern recognition systems are limited to the analysis of textural features derived from a two-dimensional (2D) image slice through the center of the tumor, despite the fact that often tumors extend to more than one slice. Thus, the exploitation of multislice volumetric features may offer additional information that will improve the accuracy of these systems.

Until now, several previous studies have employed three-dimensional (3D) textural features in pattern recognition systems for improving the discrimination accuracies attained by 2D features. In particular, a recent study [2] has shown that the calculation of 3D texture measures from low-resolution CT images might be useful in predicting microarchitectural properties of bone. In another study [3],

* Corresponding author. Tel.: +30 2610 997745.

E-mail addresses: pgeorgiadis@med.upatras.gr (P. Georgiadis), cavouras@teiath.gr (D. Cavouras).

URL: <http://mipa.med.upatras.gr/>.

intensity, gradient and anisotropy 3D textural features have been used for separating between brain MR images of controls and patients suffering from white-matter encephalopathy and/or Alzheimer's disease. Furthermore, another study [4] has found that 3D volumetric features were more sensitive and more specific than corresponding 2D features in assessing patterns of emphysema ranging from mild to severe and in distinguishing normal nonsmokers from normal smokers, while in another study [5], it has been shown that 3D features achieved higher classification accuracies when applied to lung pathology.

Regarding MRI brain tumor characterization, 2D textural features have been previously employed in pattern recognition systems for the analysis of brain lesions. More specifically, in a recent study [6] utilizing hierarchical ascending classification with correspondence factorial analysis, discrimination accuracies achieved between different tumor types ranged between 49% (tumors vs. edemas) and 63% (benign vs. malignant tumors). In another study [1], discriminant analysis and the k -nearest neighbor classifier were employed for distinguishing between brain tumors and edematous tissues, achieving maximum overall accuracy of 95%. Finally, in a previous study by our group [7], a two-level hierarchical decision tree has been employed to discriminate metastatic brain tumors from gliomas and meningiomas (primary brain tumors) using solely 2D textural features. By using a modified probabilistic neural network classifier, discrimination accuracies of 71% (metastatic vs. primary tumors) and 81% (gliomas vs. meningiomas) were achieved. On the other hand, there has only been one previous study [8] for the characterization and analysis of brain tumors employing 3D textural features extracted from MR images. The authors have shown that by using a set of six 3D co-occurrence features, instead of the 2D equivalents, and linear discriminant analysis, discrimination accuracies increased between necrosis and solid tumor (100% against 68%) and between edema and solid tumor (81% against 57%).

The aim of the present study was to extend and improve the accuracy of our previous work [7] on characterizing brain tumors

1. by designing, implementing and evaluating a pattern recognition system employing 3D textural features for improving brain tumor classification accuracies when analyzing routinely taken T_1 postcontrast MR-image series.
2. by utilizing a support vector machine (SVM)-based ensemble classification scheme along with bootstrap aggregation (bagging) at each node of a two-level hierarchical decision tree, for discriminating between metastatic and primary brain tumors at the first level and between gliomas (malignant tumors) and meningiomas (benign tumors) at the second level. These brain tumor categories were selected based on the fact that (a) brain metastasis occurs in 20% to 40% of all cancer patients while (b) meningiomas and gliomas are

the two higher incidence rated types of benign and malignant primary brain tumors [9].

3. by introducing a modified radial basis function (RBF) kernel for the SVM classifier that incorporated the least squares features transformation (LSFT) technique to improve classification accuracy.

2. Materials and methods

2.1. Data acquisition

The dataset consisted of the brain MR-image series of 67 patients with verified and untreated intracranial tumors. Patients were examined on a Siemens Sonata 1.5-T MRI Unit (Siemens, Erlangen, Germany) at the Hellenic Airforce Hospital, Greece. The dataset comprised 21 metastases, 19 meningiomas and 27 gliomas. From each case, only the T_1 -weighted postcontrast (Gadolinium) series, with spin-echo sequence, echo time (15 ms), repetition time (500 ms) and slice thickness (1.5 mm), was used for further processing. T_1 postcontrast series was chosen because it encapsulates increased diagnostic information in comparison to precontrast T_1 - or T_2 -weighted series [10]. Contrast enhancement in gadolinium-administered MRI series is intense because of the high degree of blood–brain barrier disruption. Moreover, contrast administration assists in the separation of tumor from edema, improving visualization, localization and tumor margin delineation, resulting in information-rich MR images [10].

2.2. Volume of interest extraction and feature calculation

Utilizing these MRI series, expert radiologists specified cubic volumes of interest (VOIs) within each tumor using a software program, developed for the purposes of the present study. The program was designed using the C++ programming language and the Visualization Tool Kit [11]. The developed software utilized the marching cubes algorithm [12] to build 3D models from DICOM MRI series and, thus, to provide the radiologist with a visual aid for segmenting VOIs within brain tumors (Fig. 1). Each segmented MRI-VOI was then used to calculate a set of parameters (features) that quantified properties of volume texture within the brain tumor.

Haralick et al. [13] and Galloway [14] have described a set of textural features, based on the gray-level co-occurrence and run-length matrices, which quantified textural properties of 2D images. Their 3D (volumetric) equivalents [8,15] were employed in the present study for the purpose of quantifying textural volume properties of brain tumors. In an MRI-VOI, adjacency and consecutiveness occur in each of 13 directions (compared to 4 directions in a 2D image) and, thus, 13 gray-level co-occurrence and run-length matrices were generated [8,15]. Two types of volumetric co-occurrence and run-length features were generated, the average and range of feature values over all 13 directions. Additionally, this set was enriched with features derived from the VOI's histogram (mean value, standard deviation, skewness and kurtosis).

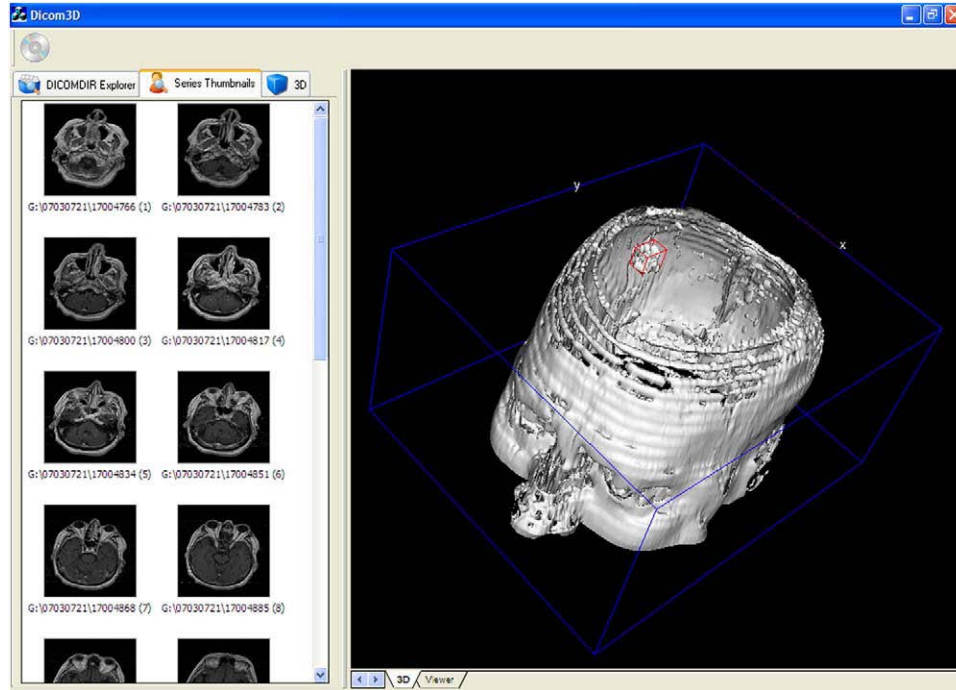


Fig. 1. Custom-made application for VOI acquisition and volumetric features extraction.

Thus, a set of 36 volumetric textural features was extracted for each brain tumor; 4 from the VOI's histogram, 22 from the co-occurrence and 10 from the run-length matrices.

All features were normalized to zero mean and unit standard deviation [16], according to Eq. (1)

$$x'_i = \frac{x_i - m}{std}, \quad (1)$$

where x_i and x'_i are the i th feature values before and after the normalization, respectively, and m and std are the mean value and standard deviation, respectively, of feature x_i over all patterns and all classes.

2.2.1. LSFT-SVM classifier

The discriminant equation of the SVM classifier [17,18] is a function of kernel $k(x_i, x)$ and is given by:

$$f(x) = \text{sign} \left(\sum_{i=1}^{N_S} a_i y_i k(x_i, x) + b \right), \quad (2)$$

where a_i are weight elements, b is a threshold parameter, x_i are support vectors (training pattern vectors with weights $a_i \neq 0$), N_S is the number of support vectors and $y_i \in \{-1, +1\}$ are class labels. For kernel $k(x_i, x)$, the Gaussian RBF [17] was employed but suitably modified by an LSFT technique. The RBF kernel function is given by:

$$k(x_i, x) = \exp \left(\frac{-||x_i - x||^2}{2\sigma^2} \right), \quad (3)$$

where σ is the standard deviation. Training patterns \mathbf{x}_i , prior to entering the RBF kernel, were transformed by means of a nonlinear LSFT technique to render classes more separable

by grouping the patterns of each class around arbitrary preselected points. The LSFT method is an extension of the linear least squares mapping technique, introduced by Ahmed and Rao [19], and it has been extended by our group in a previous study [7]. Initially, pattern vectors were extended with up to n -degree elements plus a zero-degree constant term. The dimensionality of the extended pattern vector ($\hat{\mathbf{x}}$) was equal to [16]:

$$\hat{d} = \frac{(d+n)!}{d!n!}. \quad (4)$$

Next, the pattern vectors of each class were suitably transformed so that they clustered around arbitrary selected points \mathbf{P}_i (using least squares error minimization) on the decision space of dimensionality equal to the number of classes [see Eq. (8)]. The error between a transformed vector $\mathbf{T}\hat{\mathbf{x}}_{ij}$ and point \mathbf{P}_i is:

$$\mathbf{e}_i = \mathbf{T}\hat{\mathbf{x}}_{ij} - \mathbf{P}_i \quad (5)$$

where \mathbf{T} is the transformation matrix and $\hat{\mathbf{x}}_{ij}$ is the j th extended vector of class i . In the present study, $\mathbf{P}_1=[1,0]$ and $\mathbf{P}_2=[0,1]$.

The aim was to compute \mathbf{T} , such that the total mean square error \mathbf{E} between all transformed vectors and points \mathbf{P}_i was minimized, as shown in Eq. (6):

$$\nabla_T \mathbf{E} \equiv \nabla_T \left(\sum_{i=1}^K \mathbf{e}_i \right) = 0, \quad (6)$$

where K is the number of classes.

Assuming equal a priori probabilities for each class i , Eq. (6) leads to:

$$\nabla_T \left[\sum_{i=1}^K \left(\frac{1}{N_i} \sum_{j=1}^{N_i} (\mathbf{T}\hat{\mathbf{x}}_{ij} - \mathbf{P}_i)' (\mathbf{T}\hat{\mathbf{x}}_{ij} - \mathbf{P}_i) \right) \right] = 0, \quad (7)$$

where N_i is the number of patterns of class i . Applying matrix algebra operations to Eq. (7), the transformation matrix \mathbf{T} results in:

$$\mathbf{T} = \left[\sum_{i=1}^K \left(\frac{1}{N_i} \sum_{j=1}^{N_i} \mathbf{P}_i \hat{\mathbf{x}}_{ij} \right) \right] \left[\sum_{i=1}^K \left(\frac{1}{N_i} \sum_{j=1}^{N_i} \hat{\mathbf{x}}_{ij} \hat{\mathbf{x}}_{ij}' \right) \right]^{-1}. \quad (8)$$

Transformation matrix \mathbf{T} is a $K \times \tilde{d}$ matrix; thus, the decision space dimensionality is equal to the number of classes. By applying the LSFT procedure to the RBF kernel [Eq. (3)], it is transformed as in Eq. (9):

$$k(x_i, x) = \exp \left(\frac{-\|\mathbf{T}\hat{\mathbf{x}}_i - \mathbf{T}\hat{\mathbf{x}}\|^2}{2\sigma^2} \right) \quad (9)$$

Thus, the final discriminant function of the LSFT-SVM classifier is given by:

$$f(x) = \text{sign} \left[\sum_{j=1}^{N_s} a_j v_j \exp \left(\frac{-\|\mathbf{T}\hat{\mathbf{x}}_i - \mathbf{T}\hat{\mathbf{x}}\|^2}{2\sigma^2} \right) + b \right]. \quad (10)$$

2.2.2. Bagging

Bagging, which stands for bootstrap aggregation, is another way of manipulating training data for ensemble classification schemes. In each iteration, the training subset is bootstrapped (resampled with replacement) to generate a different training subset. The logic behind bagging is that unstable classifiers, such as neural networks and decision trees, whose behavior could be significantly changed by small fluctuations in the training subset, are more likely to be stabilized after being trained with different input data [20]. Although the SVM classifier has been shown to provide a good generalization performance, the classification result of the SVM is often far from the theoretically expected level because SVM implementations usually employ approximation techniques [21]. In the present study, a bagging ensemble of three LSFT-SVMs was used to increase the discrimination accuracy of the proposed classification scheme.

2.3. Classification scheme design

An LSFT-SVM-based ensemble classification scheme (Fig. 2) was designed to discriminate between secondary (metastatic), primary benign (meningiomas) and primary malignant (gliomas) brain tumors using a two-level hierarchical decision tree. At the first level, gliomas and meningiomas were grouped into the primary brain tumor class and were classified against the metastatic brain tumor cases, while at the second level, the primary tumor

cases were further classified into cases with gliomas and meningiomas.

The external cross-validation (ECV) technique was used to avoid bias conditions [22], which may occur by using the same dataset in the feature selection and evaluation stages. Therefore, the dataset was randomly split into two subsets, one was used for optimal classifier design (2/3 of the dataset) and the other for evaluation (1/3 of the dataset). The optimum feature combination in the design stage was determined by employing the exhaustive search method [16]. Accordingly, the LSFT-SVM classifier was designed

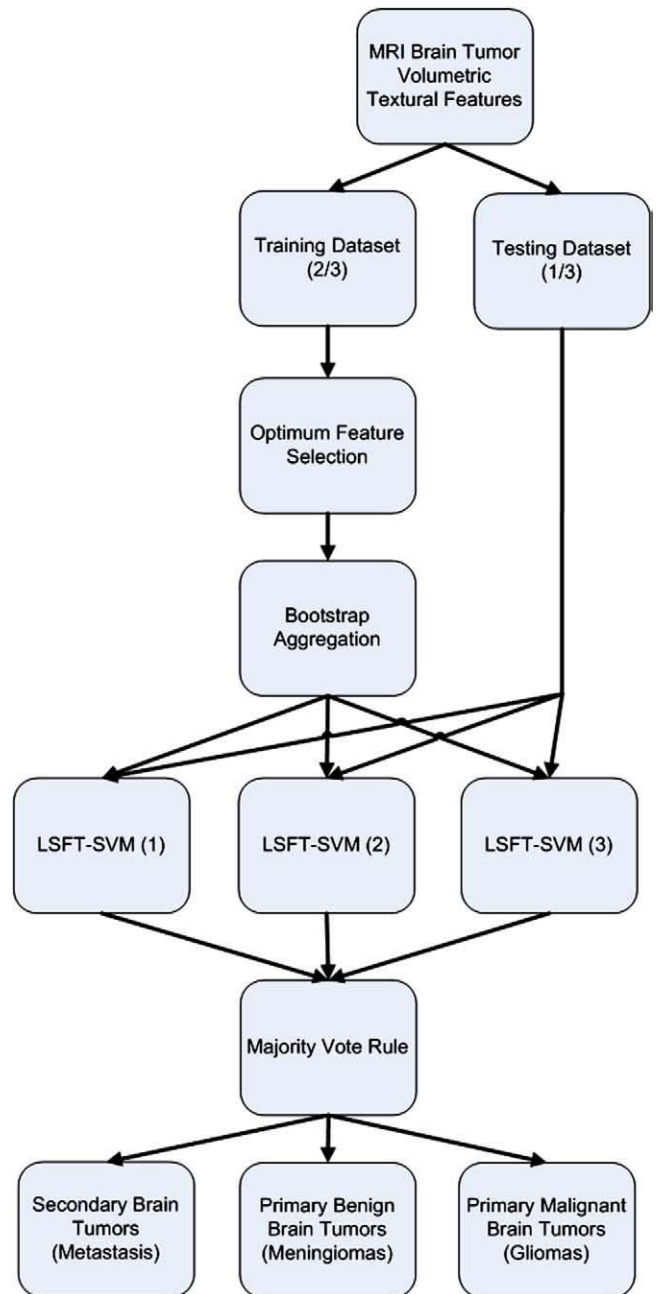


Fig. 2. Flowchart of the classification scheme utilized in the present study.

by all possible feature combinations (up to five features), and at each combination, the classifier’s performance was evaluated by means of the leave-one-out (LOO) method [16]; that is, the LSFT-SVM classifier was designed by all but one pattern vector, which was considered as unknown, and it was classified. The process was repeated, each time leaving out a different pattern vector, until all pattern vectors were classified into one of the two tumor classes. Thus, the optimal feature vector retained was the one that gave the highest classification accuracy with the least number of features (Fig. 3).

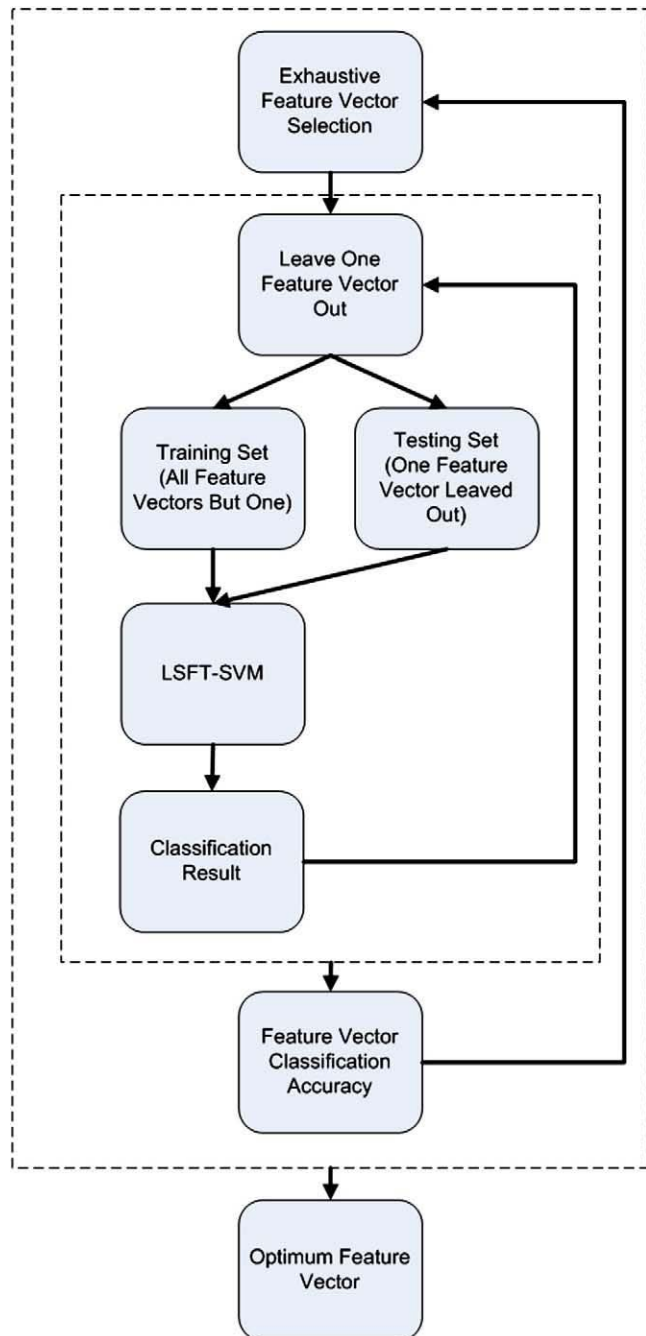


Fig. 3. Optimum feature vector combination determination procedure.

Table 1
SVM classifier truth table for discriminating primary from secondary tumors at the first tree level using 2D and 3D textural features

	Primary brain tumors	Secondary brain tumors	Accuracy (%)
	2D (3D)	2D (3D)	2D (3D)
Primary brain tumors	45 (45)	1 (1)	97.83 (97.83)
Secondary brain tumors	6 (3)	15 (18)	71.43 (85.71)
Overall accuracy			89.55 (94.03)

Next, employing the optimal feature vector, the design dataset was bootstrapped (resampled with replacement) according to the bagging technique three times and an equal number (3) of LSFT-SVM classifiers was designed. An implementation of the Mersenne twister random number generation engine was used to ensure that patterns in each bootstrapped sample were selected randomly [23]. That ensemble classifier design was next utilized to classify the evaluation subset. The output of each LSFT-SVM classifier was used in the formulation of a collective decision using the majority vote rule [24]. Thus, the output of the system was expressed as in Eq. (11).

$$\sum_{i=1}^r D_{ji} = \max_{k=1}^K \sum_{i=1}^r D_{ki}, \quad (11)$$

where r is the number of classifiers and D_j is a binary decision value for the j th class. The whole design and evaluation (ECV) procedure was repeated 10 times, and the classification results were averaged. Apart from the linear (first degree) procedure, the quadratic (second degree) LSFT procedure was also employed to investigate the classification accuracy behavior of the proposed LSFT-SVM classifier as higher-degree nonlinear elements were introduced in its discriminant function.

Prior to classifying volumetric textural features with the proposed classification scheme, comparison was performed between the discrimination efficiency of 2D and 3D textural features at both levels of the decision tree. The central slice of the each VOI was used to calculate the 2D co-occurrence and run-length matrices to extract the 2D textural features.

Table 2
Comparative classification results between 2D and 3D textural features employing the SVM classifier at both levels of the decision tree

Number of features	First level: primary vs. metastatic tumors, overall accuracy (%)		Second level: malignant vs. benign tumors, overall accuracy (%)	
	2D textural features	3D textural features	2D textural features	3D textural features
1	73.13	76.12	93.48	93.48
2	82.09	83.58	95.65	95.65
3	86.57	89.55	95.65	97.83
4	88.06	91.04	97.83	100
5	89.55	94.03	100	100

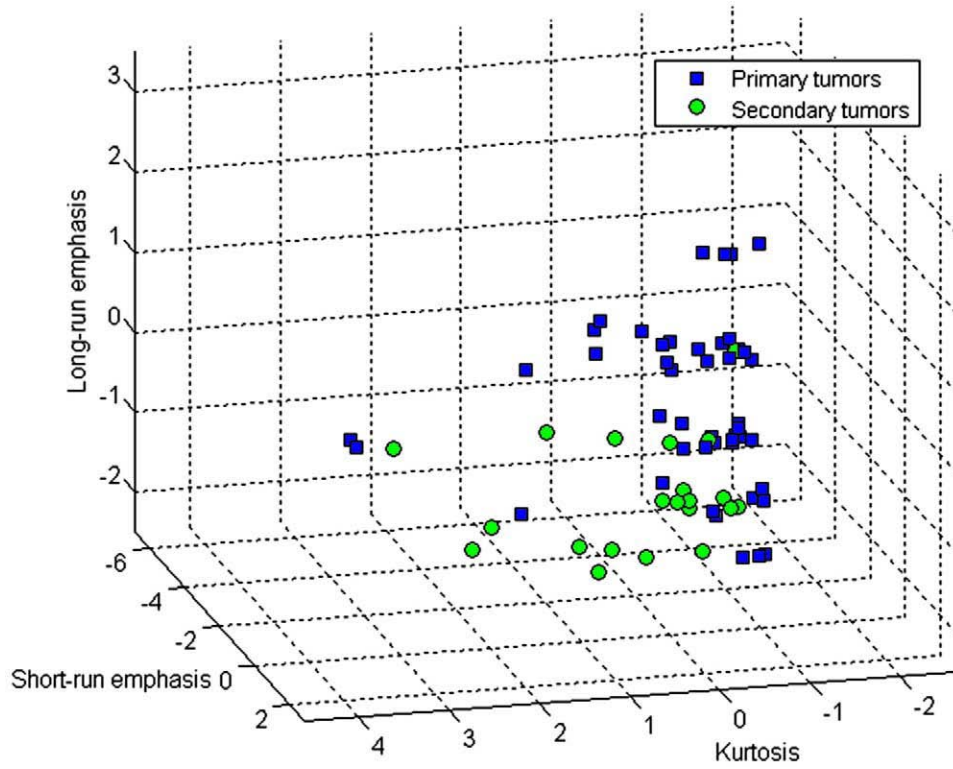


Fig. 4. Scatter diagram of the primary and secondary tumors utilizing 3D textural features (kurtosis, short-run emphasis, long-run emphasis).

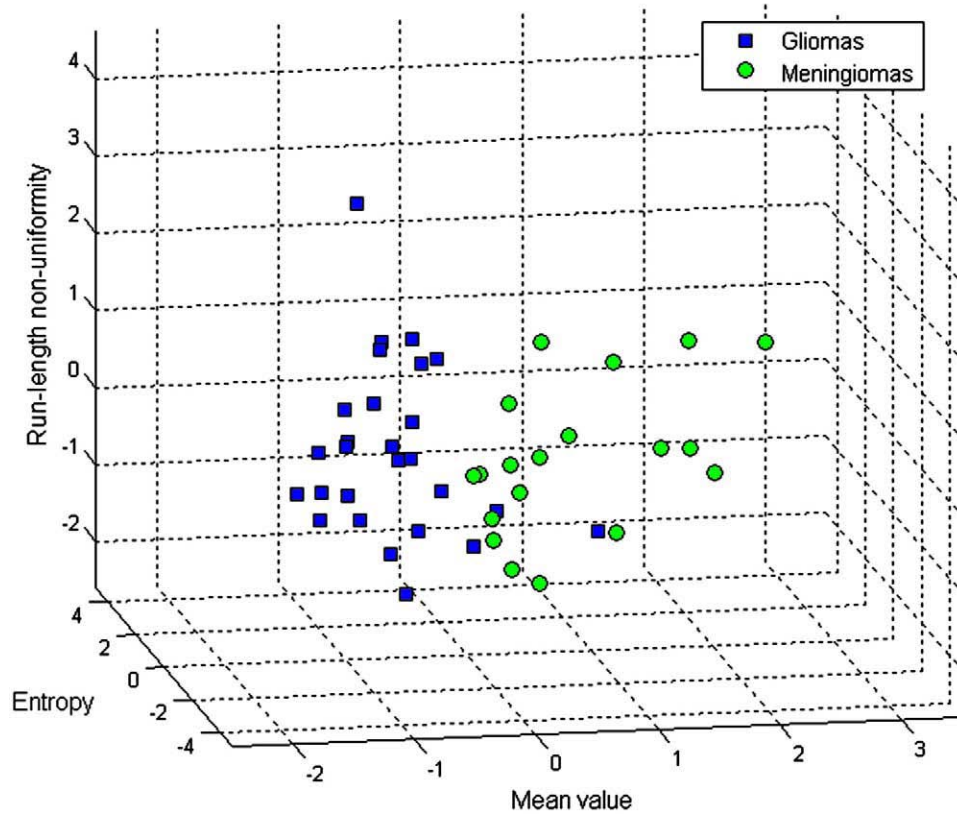


Fig. 5. Scatter diagram of cases with gliomas and meningiomas employing 3D textural features (mean value, entropy and run-length nonuniformity).

Table 3
Comparative classification results employing the linear and the quadratic LSFT-SVM classifiers for both levels of the decision tree

Number of features	First level: primary vs. metastatic tumors, overall accuracy (%)		Second level: malignant vs. benign tumors, overall accuracy (%)	
	Linear LSFT	Quadratic LSFT	Linear LSFT	Quadratic LSFT
1	73.13	77.61	91.30	93.48
2	80.60	82.09	95.65	95.65
3	83.58	91.04	97.82	100
4	88.06	95.52	97.82	100
5	88.06	97.01	100	100

Thus, the following 2D features were extracted: 4 features from the slice’s histogram, 22 from the co-occurrence matrices and 10 from the run-length matrices. The classification accuracies of both 2D and 3D features were evaluated employing the LOO method for all, up to five, possible feature combinations.

3. Results

To assess the discrimination efficiency of volumetric features as compared to 2D features, we performed a comparative evaluation at both levels of the decision tree using the SVM classifier.

At the first level, the overall classification accuracy employing 2D textural features was 89.55%, employing skewness, correlation, difference entropy, gray-level non-uniformity and run-length nonuniformity features combination. Individual accuracies in discriminating between primary and secondary brain tumors were 97.83% and 71.43%, respectively (Table 1). Best 2D feature vector, used for the optimal design of the SVM classifier, comprised skewness, correlation, difference entropy, gray-level non-uniformity and run-length nonuniformity. 3D features increased overall classification accuracy to 94.03% using the same classifier. The individual accuracies were 97.83% and 85.71%, respectively (Table 1). The best volumetric feature vector comprised standard deviation, kurtosis, angular second moment, contrast and long-run emphasis. Comparative classification results for various numbers of features and for both tree levels, employing 2D and 3D features, are presented in Table 2. Fig. 4 is a scatter diagram of the primary and secondary tumor cases using 3D textural features.

At the second level of the decision tree, both 2D and 3D features achieved 100% discrimination accuracy between primary benign and malignant tumors. Fig. 5 is a scatter diagram of cases with gliomas and meningiomas employing 3D textural features.

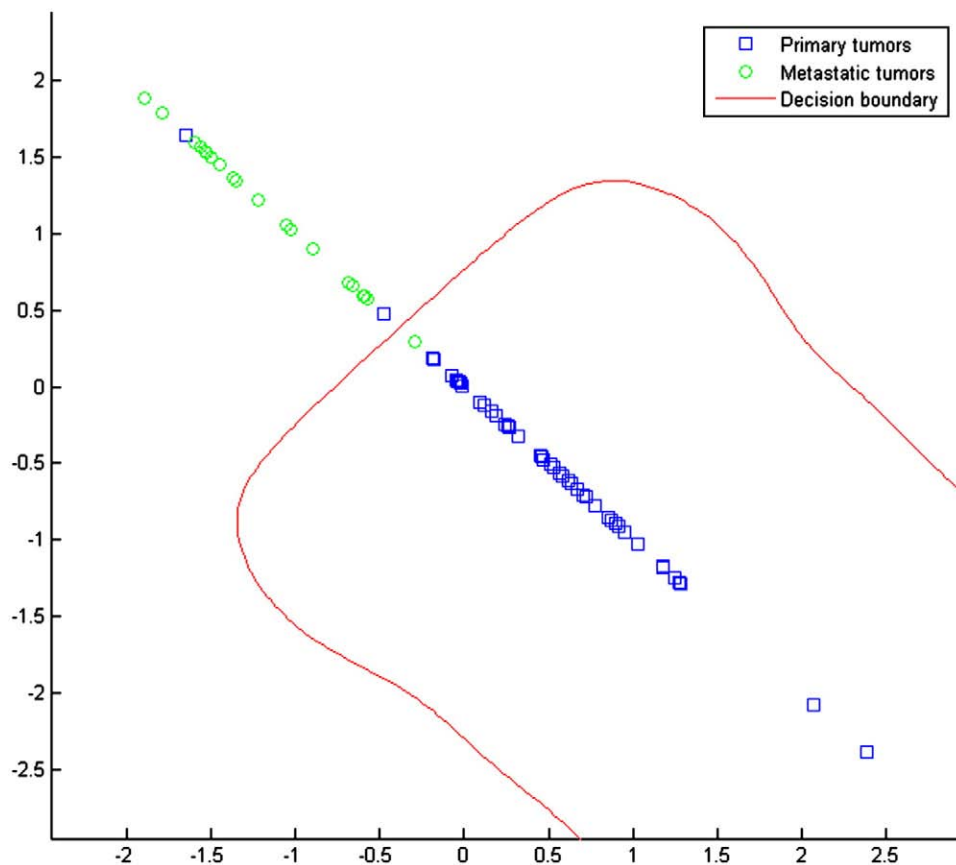


Fig. 6. Decision space scatter diagram of the optimum five-feature combination of the quadratic LSFT-SVM classifier and the corresponding decision boundary for discriminating primary from metastatic tumors employing 3D textural features.

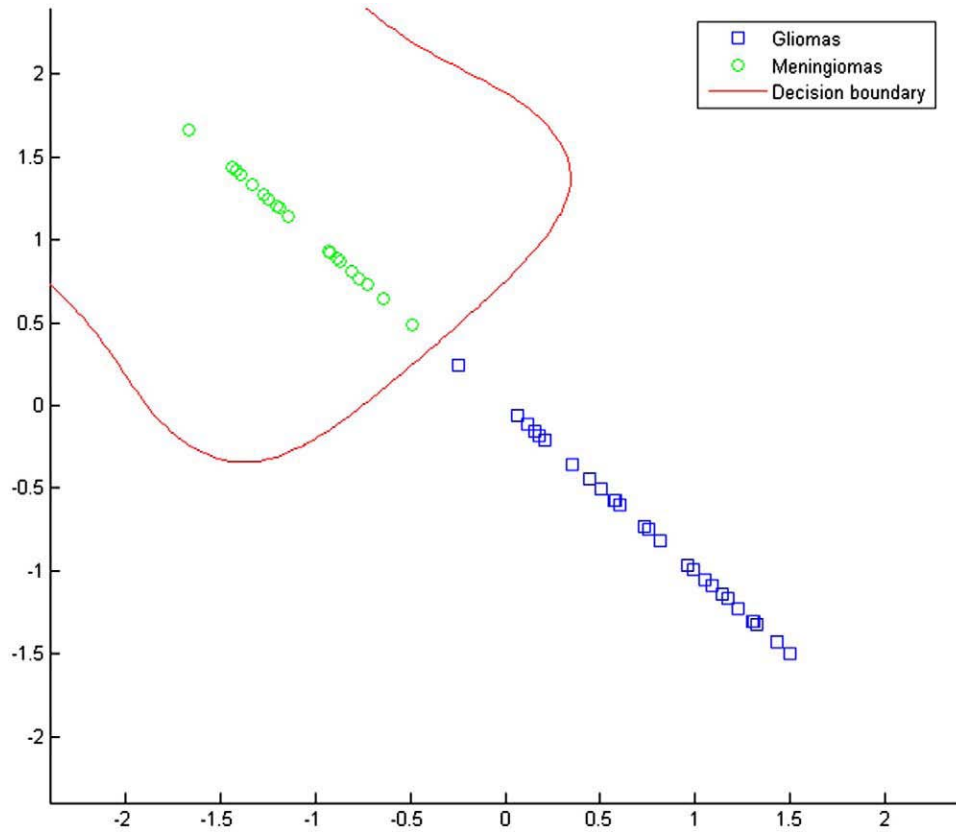


Fig. 7. Decision space scatter diagram of the optimum five-feature combination of the quadratic LSFT-SVM classifier and the corresponding decision boundary for discriminating gliomas from meningiomas employing 3D textural features.

To further enhance volumetric feature classification accuracies, the linear and the quadratic LSFT-SVM classifiers were employed at both levels of the decision tree. The overall classification accuracies at the first level of the decision tree employing the linear and the quadratic LSFT-SVM classifier were 88.06% and 97.01%, respectively (Table 3). At the second level, the classification accuracy for both first and second degree LSFT-SVM was 100% (Table 3). Figs. 6 and 7 show the scatter diagrams of the decision space along with the corresponding decision boundaries for primary and secondary tumors and for benign and malignant tumors, respectively, using the quadratic LSFT-SVM classifier. The decision boundary of the LSFT-SVM is a line that partitions the decision space into regions,

one for each class, satisfying the equality $f(x)=0$ [see Eq. (10)]. The classifier then assigns all the points on one region of the decision boundary as belonging to one class and all those on the other region as belonging to the other class.

The overall classification accuracy at the first level of the decision tree using three bootstrap aggregated quadratic LSFT-SVM classifiers was 98.51% (Table 4). Best feature vector, used for the optimal design of the classification system, comprised the skewness, kurtosis, inverse difference moment, difference variance and run percentage. Regarding the second level of the decision tree, all glioma and meningioma cases were correctly classified, resulting in 100% overall classification accuracy. The optimal feature

Table 4
Classification results employing the LSFT-SVM ensemble classifier scheme (bagging)

Number of features	Primary vs. metastatic tumors, overall accuracy (%)	Malignant vs. benign tumors, overall accuracy (%)
1	82.09	93.48
2	91.04	95.65
3	94.03	97.83
4	97.01	100
5	98.51	100

Table 5
Classification results utilizing the ECV method and the LSFT-SVM ensemble classifier scheme (average and standard deviation after 10 ECV repetitions)

Number of features	Primary vs. metastatic tumors, overall accuracy (%)	Malignant vs. benign tumors, overall accuracy (%)
1	67.27±2.03	90.67±3.65
2	71.82±2.03	92±5.58
3	79.09±2.49	93.33±4.71
4	84.55±2.49	96±3.65
5	88.18±2.49	97.33±2.65

vector comprised the mean value, kurtosis, correlation, difference variance and run-length nonuniformity.

By employing the ECV method for assessing the generalized performance of the system, the mean overall classification accuracy at the first level of the decision tree was 88.18%. At the second level of the decision tree, the mean overall accuracy for discriminating between gliomas and meningiomas was 97.33% (Table 5).

The overall accuracies of the classification system in discriminating metastatic tumors from gliomas and meningiomas can be obtained by multiplying the corresponding accuracies achieved at each level of the decision tree [16]. Consequently, by employing the ECV method, the classification accuracies were 77.14% for the metastatic tumors, 89.19% for gliomas and 93.33% for meningiomas.

4. Discussion

An essential outcome of this study is that 3D features have significantly improved classification accuracy in discriminating primary from metastatic tumors as compared to 2D features (improvement from 89.55% to 94.03%). Such a significant improvement was not observed for the discrimination of benign from malignant tumors, since both 2D and 3D features have resulted in 100% accuracy.

The reason for selecting only the central slice of the VOI in order to extract 2D textural features was to comply with the methodology followed by most previous studies [1,6]. In this way, we could emphasize the benefits of using 3D textural features, which code information from the whole VOI, compared to selecting just one slice and extracting 2D features from this slice. However, it has to be pointed out that high classification accuracies achieved by 3D texture metrics might be due to the fact that 3D features exploit additional information derived from all available slices (and not just the central slice).

Another important conclusion is that the utilization of LSFT-SVM ensemble classifier scheme further improved classification accuracy as compared to using individual SVM classifiers (the SVM or the linear LSFT-SVM) for both levels of the decision tree. More specifically, at the first level of the decision tree, improvement was from 97.01% to 98.51%, with only one metastatic tumor misclassified. At the second level, all gliomas and meningiomas were correctly assigned to the proper class (100% accuracy). The enhanced performance of the LSFT-SVM ensemble classifier scheme might be attributed to the increased class separability that the LSFT procedure provides when nonlinear terms were introduced in the classifier's discriminant function. A worth-mentioning characteristic of the LSFT method is that the classification problem is reduced to two dimensions regardless of the dimensionality of the input feature space.

Features that optimized classification results of the ensemble scheme at the first level of the decision tree encoded information related to the distribution asymmetry around the mean gray-tone value (skewness), the gray-tone distribution sharpness as compared to the normal distribution

(kurtosis), the degree of homogeneity (inverse difference moment), the amount of randomness (difference variance) and measures of the linear structures appeared in the VOI (run percentage). At the second level of the decision tree, the optimum features described the gray-tone linear dependencies (correlation), the dispersion of the gray-tone intensity values (sum average), the variance of the normalized gray tones in the spatial domain (sum variance) and the degree of homogeneity of the VOI (inverse difference moment, run-length nonuniformity). Some of these textural characteristics are related to textural parameters that physicians employ in diagnosis [6] and they are proportional to the textural imprint of brain tumors; that is, gliomas have heterogeneous texture while meningiomas appear to be homogeneous in MRI.

The ECV method enabled us to assess the generalization of the system to new "unseen" data. Under the ECV, the LSFT-SVM ensemble classifier scheme achieved accuracy of 88.18% and 97.33% at the first and second level of the decision tree, respectively. Moreover, for comparative purposes, the system was constructed using the SVM classifier without the LSFT technique and without feature reduction. Results have shown an inferior performance of the system with 80.64% and 90.32% at the first and second level of the decision tree, respectively. Feature reduction enabled the elimination of features with poor discrimination accuracy, whereas LSFT improved class separability, enhancing in this way the overall classification performance of the system. Thus, results using the LSFT-SVM ensemble system indicate that the proposed method might be used for accurate discrimination of benign, malignant and metastatic brain tumors. The latter is of crucial importance. Primary and metastatic tumors follow different treatment protocols (radiation therapy and chemotherapy for metastatic tumors while primary tumors may also require surgical intervention [25,26]). Moreover, malignant tumors, according to their grade, may require specific postsurgery treatment such as external beam radiotherapy or chemotherapy [27] while benign tumors may require stereotactic radiosurgery [28].

Considering the results of the present study, the proposed classification system constructed with 3D textural features achieved higher accuracies than those obtained in previous studies that have used solely 2D features. In particular, in a previous study by our group [7], using the same brain tumor categories and an LSFT-modified probabilistic neural network and the ECV technique, discrimination accuracies of 71.43% for the metastatic tumors, 72.22% for gliomas and 81.25% for meningiomas have been achieved. The present study improved these accuracies to 77.14% for the metastatic tumors, 89.19% for gliomas and 93.33% for meningiomas, employing the ECV method. In another study by our group [29], direct discrimination between metastatic, malignant and benign tumors resulted in classification accuracies of 87.50%, 96.67% and 95.24%, respectively, employing only the LOO technique. The classification scheme utilized in the present study, employing the LOO method, achieved classification accuracies of 95.24% for the metastatic tumors and 100% for

both gliomas and meningiomas. The main differences of the present study compared to our previous studies [7,29] are (a) the inclusion of 3D textural features, (b) the extension of the method by utilizing the bagging ensemble technique, (c) the introduction of a modified RBF kernel for the SVM classifier that incorporated the LSFT technique and (d) the improvement of results in discriminating metastatic, benign and malignant tumors.

Moreover, in a recent study [30], an SVM-based classification system discriminated gliomas and meningiomas with 95% overall accuracy, employing as features image intensities from four MR sequences (T_1 , T_2 , PD and GD). When features derived from MR spectroscopy were also included, classification accuracy reached 99.8%. In another study [31], employing the LS-SVM classification algorithm and MR spectroscopic data, overall accuracies in distinguishing between secondary brain tumors and meningiomas or glioblastomas or astrocytomas were 97%, 59% and 96%, respectively. Our findings are comparable, however, employing solely volumetric textural features from the T_1 contrast-enhanced MRI series.

The computational time required for the training and evaluation procedures were approximately 11 h for the proposed classification system. This time-demanding computational load is attributed to the iterative methods used for best feature selection (exhaustive search) and for system's evaluation (ECV, LOO, optimal classifier's design and parameter estimation). However, once the system has been designed, no iterative processes are required in order to classify a new case. Thus, classification of new cases is instantaneous.

5. Conclusion

The utilization of 3D textural features improved accuracy in the characterization of brain tumors on volumetric MR images as compared to using 2D textural features. LSFT-SVM ensemble classifier scheme further enhanced classification results. The proposed system might be used as an assisting tool for brain tumor characterization on volumetric MR images.

Acknowledgments

Funding by the University of Patras Research Committee under the basic research program "K. Karatheodori," project title "Computer-Assisted Diagnosis of Brain Tumors Based on Statistical Methods and Pattern Recognition Techniques," is gratefully acknowledged.

References

- [1] Lerski RA, Straughan K, Schad LR, Boyce D, Bluml S, Zuna I. MR image texture analysis — an approach to tissue characterization. *Magn Reson Imaging* 1993;11:873–87.
- [2] Showalter C, Clymer B, Richmond B, Powell K. Three-dimensional texture analysis of cancellous bone cores evaluated at clinical CT resolutions. *Osteoporos Int* 2006;17:259–66.
- [3] Kovalev VA, Petrou M, Bondar YS. Texture anisotropy in 3-D images. *IEEE Trans Image Proc* 1999;8:346–60.
- [4] Xu Y, Sonka M, McLennan G, Guo J, Hoffman E. Sensitivity and specificity of 3-D texture analysis of lung parenchyma is better than 2-D for discrimination of lung pathology in stage 0 COPD. *Proceedings of the medical imaging 2005: physiology, function, and structure from medical images*; 2005. p. 474–85.
- [5] Xu Y, van Beek E, Hwanjo Y, Guo J, McLennan G, Hoffman AE. Computer-aided classification of interstitial lung diseases via MDCT: 3D adaptive multiple feature method (3D AMFM). *Acad Radiol* 2006;13:969–78.
- [6] Herlidou-Meme S, Constans JM, Carsin B, Olivie D, Eliat PA, Nadal-Desbarats L, et al. MRI texture analysis on texture test objects, normal brain and intracranial tumors. *Magn Reson Imaging* 2003;21:989–93.
- [7] Georgiadis P, Cavouras D, Kalatzis I, Daskalakis A, Kagadis GC, Sifaki K, et al. Improving brain tumor characterization on MRI by probabilistic neural networks and non-linear transformation of textural features. *Comput Methods Programs Biomed* 2008;89:24–32.
- [8] Mahmoud-Ghoneim D, Toussaint G, Constans JM, de Certaines JD. Three dimensional texture analysis in MRI: a preliminary evaluation in gliomas. *Magn Reson Imaging* 2003;21:983–7.
- [9] Doolittle ND. State of the science in brain tumor classification. *Semin Oncol Nurs* 2004;20:224–30.
- [10] Runge V. *Clinical MRI*. Philadelphia: Saunders; 2002.
- [11] Schroeder WJ, Schroeder WJ, Avila LS, Hoffman W. Visualizing with VTK: a tutorial. *IEEE Comput Graph Appl* 2000;20:20–7.
- [12] Lorensen W, Cline H. Marching cubes: a high resolution 3D surface construction algorithm. *Comput Graph* 1987;21:163–9.
- [13] Haralick RM, Shanmugam K, Dinstein I. Textural features for image classification. *IEEE Trans Syst Man Cybern* 1973;SMC-3:610–21.
- [14] Galloway MM. Texture analysis using grey level run lengths. *Comp Graph Image Proc* 1975;4:172–9.
- [15] Xu DH, Kurani A, Furst J, Raicu D. Run-length encoding for volumetric texture. *Proceedings of the 4th IASTED International Conference on Visualization, Imaging, and Image Processing — VIIP 2004*; 2004. p. 6–8.
- [16] Theodoridis S, Koutroumbas K. *Pattern recognition*. New York: Academic Press; 1999.
- [17] Kecman V. *Learning and soft computing, support vector machines, neural networks, and fuzzy logic models*. Cambridge: MIT Press; 2001.
- [18] Muller KR, Mika S, Ratsch G, Tsuda K, Scholkopf B. An introduction to kernel-based learning algorithms. *IEEE Trans Neural Netw* 2001;12:181–201.
- [19] Ahmed N, Rao R. *Orthogonal transforms for digital signal processing*. New York: Springer-Verlag; 1975.
- [20] Breiman L. Bagging predictors. *Machine Learning* 1996;24:123–40.
- [21] Kim HC, Pang S, Je HM, Kim D, Bang SY. Support vector machine ensemble with bagging. *Lect Notes Comput Sci* 2002;2388:131–41.
- [22] Ambrose C, McLachlan GJ. Selection bias in gene extraction on the basis of microarray gene-expression data. *Proc Natl Acad Sci U S A* 2002;99:6562–6.
- [23] Makoto M, Takuji N. Mersenne twister: a 623-dimensionally equidistributed uniform pseudo-random number generator. *ACM Trans Model Comput Simul* 1998;8:3–30.
- [24] Kittler J, Hatef M, Duin RPW, Matas J. On combining classifiers. *IEEE Trans Pattern Anal Mach Intell* 1998;20:226–39.
- [25] Peacock K, Lesser G. Current therapeutic approaches in patients with brain metastases. *Curr Treat Options Oncol* 2006;7:479–89.
- [26] Graham CA, Cloughesy TF. Brain tumor treatment: chemotherapy and other new developments. *Semin Oncol Nurs* 2004;20:260–72.
- [27] Andratschke N, Grosu AL, Molls M, Nieder C. Perspectives in the treatment of malignant gliomas in adults. *Anticancer Res* 2001;21:3541–50.

- [28] Lunsford LD. Contemporary management of meningiomas: radiation therapy as an adjuvant and radiosurgery as an alternative to surgical removal? *J Neurosurg* 1994;80:187–90.
- [29] Georgiadis P, Cavouras D, Kalatzis I, Daskalakis A, Kagadis G, Sifaki K, et al. Non-linear least squares features transformation for improving the performance of probabilistic neural networks in classifying human brain tumors on MRI. *Lect Notes Comput Sci* 2007;4707:239–47.
- [30] Devos A, Simonetti AW, van der Graaf M, Lukas L, Suykens JA, Vanhamme L, et al. The use of multivariate MR imaging intensities versus metabolic data from MR spectroscopic imaging for brain tumour classification. *J Magn Reson* 2005;173:218–28.
- [31] Devos A, Lukas L, Suykens JA, Vanhamme L, Tate AR, Howe FA, et al. Classification of brain tumours using short echo time 1H MR spectra. *J Magn Reson* 2004;170:164–75.